Magnetic Studies of VSe, $CrSb_{1.05}$, and Copper Substituted Magnesium Ferrite

By Austen Hsiao
June, 2019

In partial fulfillment of the requirements for the degree of MS in Chemistry

1. Magnetism Background

Magnetic materials can be classified as either diamagnetic or paramagnetic. In the case of diamagnetism, no magnetic response is observed due to complete pairing of all electrons in occupied orbitals. Conversely, paramagnetism occurs in the event that at least one unpaired electron exists. Paramagnetic structures are characterized by randomly oriented spins, caused by thermal energy in which no overall magnetic response is observed. However, the spins can be aligned by the application of an external magnetic field. Spontaneous ordering is also possible within paramagnetic materials. If all unpaired spins are oriented in the same direction, it is said to be ferromagnetic. In the case where unpaired spins are oriented anti-parallel to each other, such behavior is so called antiferromagnetic. Ferrimagnetism refers to the phenomenon in which the magnitude of anti-parallel spins do not completely cancel out, resulting in some remnant magnetism. In cases involving conductors, the contribution to magnetism by delocalized spins may result in what is called Pauli paramagnetism. "Free" electrons in a conducting material are affected by the magnetic field; resulting in an increased number of electrons aligned antiparallel to the field compared to parallel spins. As temperature increases, the delocalized spins are relatively unaffected and will exhibit an increased degree of ordering.

Spontaneous ordering is explained by the Kramers-Anderson model of superexchange. Orbital overlap between magnetic and non-magnetic ions in a M(magnetic)-N(non-magnetic)-M fashion where orbitals of the magnetic ion are half filled, can result in both magnetic ions either being spin ordered parallel, resulting in ferromagnetism (FM), or antiparallel, resulting in antiferromagnetism (AFM). The non-magnetic ion facilitates ordering. Bond angle can be used to predict behavior. 90^o interactions and 180^o interactions between M-N-M bonding produces FM and AFM type, respectively. Bonding angles of either ~60^o or ~120^o cannot be predicted.[1]

The most common approach to viewing magnetic data is a plot of molar susceptibility (χ, emu/mol) versus temperature (K). This data can be collected either in zero field cooling or with an applied field. Susceptibility may be explained as the magnitude of response of the spins at a given temperature—high susceptibility suggests high degree of spin ordering. Thus, we can expect certain profiles for magnetic type materials. For diamagnets, the susceptibility should be zero or negative due to no magnetic moment of the material and should remain independent of temperature. Ferromagnetic materials are indicated by a half-parabolic profile with a maximum susceptibility at a temperature of 0 K—spins remain ordered up to a critical temperature referred to as the Curie temperature. Antiferromagnets exhibit low susceptibility at both low and high temperatures with a peak at the Neel temperature. Prior to the Neel temperature, antiferromagnets have a mostly linear relationship between χ and T, while after the Neel temperature, a 1/T relationship is observed. Paramagnets should exhibit a 1/T relationship owing to thermal vibrations at high temperatures inhibiting ordering; likewise, a maximum susceptibility should be observed near 0 K; it should be noted that this maximum is typically much lower than ordered magnetic types.

With paramagnetic profiles, a graph of inverse susceptibility versus temperature produces the Curie-Weiss (CW) plot. Due to the overall 1/T relationship in the susceptibility versus temperature graph, the Curie-Weiss plot is linear, paramagnetic profiles are thus said to follow Curie-Weiss behavior. This linear line can be extrapolated back to the x-intercept to determine the Curie-Weiss constant, whose sign enables us to determine the short-range magnetic

interactions. A positive CW constant indicates short range ferromagnetism, 0 K CW constant indicates complete paramagnetism, and a negative value indicates short range antiferromagnetism. The magnetic response in antiferromagnetic materials after the Neel temperature also follows Curie-Weiss behavior—in such cases, short range ordering can also be determined by the CW plot. From the CW constant, an additional 'frustration parameter' can be calculated. In frustrated antiferromagnetic structures where the interacting spins of adjacent atoms are not trivial, the absolute value of the CW constant taken upon the Neel transition temperature calculates 'f', the frustration parameter. As an arbitrary threshold, a frustration value above 10 indicates a highly frustrated structure. This parameter is used as a way to quantify an otherwise qualitative factor.

With all of these considerations in mind, magnetic measurements can be used for more than just direct property measurements, but to also determine the presence of other properties such as superconductivity. The author's studies in magnetic structure-property relationships has enabled the investigation of three separate chemical systems: VSe, $CrSb_{1.05}$, and copper substituted magnesium ferrite.

2. VSe

Background

Vanadium selenide was originally studied for its magnetic property by Tsubokawa in 1959.[2] Approximately ten years prior to this publication, the Kramers-Anderson model was proposed as the method of spontaneous magnetization through what is now known as the Kramers' (or Kramers-Anderson model) model for superexchange.[3] Tsubokawa's publication sought to elucidate the magnetic behavior of the early 3d transition-metal chalcogenides. Tsubokawa rationalized the antiferromagnetic behavior in his sample to the Kramers model. Furthermore, the data presented in the original study suggest a highly frustrated structure with an ordering peak at 160 K. The CW constant for Tsubokawa's VSe sample was found to be approximately -2500 K; the subsequent frustration parameter is thus ~16. This type of structure, which orders but has a highly frustrated lattice, is unconventional and should be studied for its fundamental knowledge. Recent advances in frustrated structures have spurred new research in thin film design.[4,5] While the application of frustrated thin films has yet to be realized, this field is still in its infant stages. The application of many historical devices such as $SrTiO_3$ and $BaTiO_3$ began very differently than what they are commonly known for in the present time.[6]

Experimental

Two samples of VSe were prepared by the conventional solid-state method. Powders of vanadium and selenium were manually ground in an agate mortar and pestle for 10 minutes to ensure adequate grain size for a complete reaction. Due to the potential of vanadium to oxidize in air and the volatility of selenium, both samples were sealed into evacuated silica tubes. The first sample was heated at 950^{o}C for 12 hours while the second sample was heated at 1000^{o}C for 168 hours. Both samples utilized a 2^{o}/min heating and cooling rate to encourage crystallinity. The purpose for the drastic difference in heating times is twofold: we address the possibility of the 12-hour sample not being completely reacted and possibly increase the crystallinity of sample 2.

Samples were characterized using a benchtop Rigaku miniflex diffractometer and CuKα x-ray source. A zero-background silicon crystal sample holder was used during XRD data collection for higher resolution.

Our samples were sent to Dr. Arthur Ramirez at UC Santa Cruz for MPMS measurements.

Results/Discussion

Whole pattern fitting of the XRD patterns confirmed the $P6_3/mmc$ space group as found by Tsubokawa. All peaks within the pattern belong to this majority phase and impurities were not detected by this method. Figure 1 presents the XRD pattern for both samples. Sample 2, which was heated for 168 hours at 1000ºC had no noticeable difference when compared to sample 1, suggesting a complete reaction within 12 hours at 950ºC.

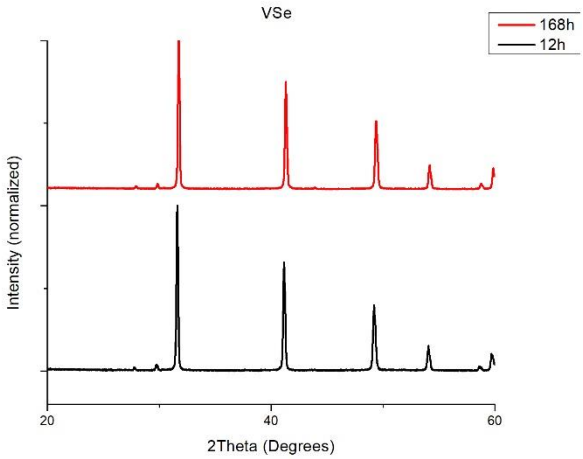

Figure 1: Two VSe samples. Red shows sample heated at 1000ºC for 168h. Black line shows sample heated at 950ºC for 12h. Negligible difference suggests complete crystal formation in sample 1

Magnetic measurements for both samples revealed interesting results that are inconsistent with the original publication. While Tsubokawa's VSe sample is very clearly antiferromagnetic with a distinct ordering peak at 160 K, both of our samples follow more paramagnetic behavior. Sample 1 seems to have a small peak near 160 K, but upon enhancing the data as seen in figure 2, it is uncertain whether this peak is the result of antiferromagnetic ordering or minor amounts of impurities. In fact, there is an additional peak at higher temperature in both samples. In order to elucidate this problem, higher resolution x-ray data should be collected and refined. Even so, the level of impurities causing effects on the magnetic property may be undetectable by XRD. The Curie-Weiss constant for sample 1 is found to be approximately 2600 K, leading to a frustration parameter of 18. This is in contrast to Tsubokawa's sample which had a frustration parameter of 16. It is possible that the frustrated lattice is simply too frustrated to allow ordering. However, if this is the case, a more crystalline material would decrease the frustration parameter; as we see in the second sample, the frustration parameter maintains its value of 18. This suggests that either antiferromagnetic ordering is not occurring or our heating method did not improve crystallinity.

Tsubokawa cites the Kramer's model as the mechanism for providing AFM behavior, however, the electronic consideration of the magnetic ion disproves this notion. The 2+ oxidation state of vanadium allows for 3 3d electrons. In the hexagonal lattice, VSe cannot exhibit superexchange via the Kramer's model because overlap of half-filled d-orbitals of vanadium and p-orbitals of selenium cannot occur. Only the t_{2g} (d_{xy}, d_{xz}, d_{yz}) orbitals, which fill space between the axes of V-Se bonding, are occupied, indicating that only metal-metal interaction is present. The vanadium e_g orbitals would need to be partially filled for possible superexchange.

We can consider the bonding of vanadium (II) oxide to further support our claim. Although VO exists in the NaCl structure type (compared to NiAs structure of VSe), the similar metal oxidation state means that no superexchange occurs—the 3d electrons exist between the bonding

axes and contribute only to d-d orbital overlap between metals. VO has a metal-metal distance of 2.89 Å and exhibits intermediate magnetic properties, that is, between AFM and FM behavior.[7] VSe has a metal-metal distance of 2.99 Å which means that the d-orbitals are further apart, decreasing interaction.

In conjunction with the data for VO, the increase in susceptibility we see in our samples at low temperatures may be the result of some remnant magnetization. This profile could be due to intermediate magnetic behavior, but the tail at low temperature appears more paramagnetic than ferromagnetic. If the increase in susceptibility is indeed caused by ferromagnetic ordering, spin canting may be the culprit, providing a small ferromagnetic response. Without higher resolution data to determine sample purity, it is difficult to provide definitive evidence for either case.

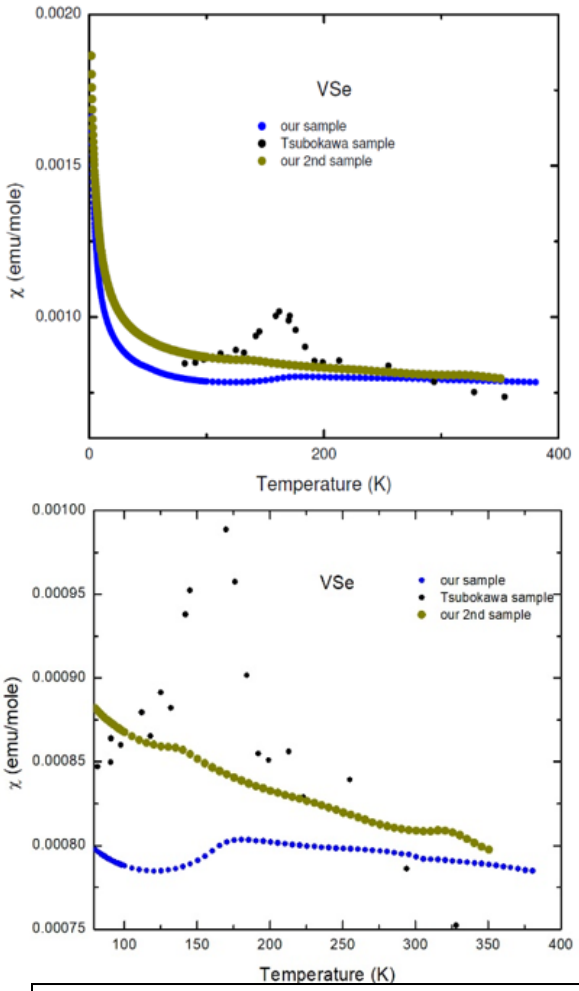

Figure 2: Magnetic data for VSe samples. (Top) Antiferromagnetic ordering peak is seen for Tsubokawa's sample at 160 K while a lack of ordering is observed for our samples. Small peaks in this region may be due to impurities or a sign of weak ordering. (Bottom) Zoomed-in diagram

3. $CrSb_{1.05}$

Background

$CrSb_{1.05}$ was first investigated by Dahal et. al. in 2017.[8] Superconducting materials are used in more high-tech applications for such use as mag-lev trains, MRI machines, NMR spectroscopy, and high-speed data transfer. These applications, however, can be expensive, due to the need for liquid gases to achieve the superconducting state, which is generally near absolute zero. Thus, research in this field is important to find high temperature superconductors (SC). As it stands, the requirements for designing SCs is unknown. Attempts at finding correlations between structural properties and a SC state is currently the best method for innovation.

The defining aspect consistent among copper oxide SCs is the presence of spin stripe ordering.[9–11] This is a phenomenon in which spins in the x-y plane are ferromagnetically ordered while spins along the z-axis are ordering antiferromagnetially. This results in a structure of layered spins where the overall magnetic behavior is antiferromagnetic.

Dahal et. al. provides evidence for possible superconductivity, but fails to test for the Meissner effect. This effect is the ability of a SC to expel any applied magnetic field; surface currents negate any incoming field. There are two types of SCs: type 1 exists in the SC state until an applied field overpowers spontaneous field expulsion; type 2 exists in the SC state until a critical applied field at which point vortex states are created. Vortex states allow penetration of magnetic field at

certain points in the material. At the second critical applied field, the weakened Meissner effect breaks and the SC state is broken.

BCS (Bardeen–Cooper–Schrieffer) theory defines the mechanism for superconductivity. In conventional materials, inconsistencies within the lattice (i.e. defects, thermal movement, etc.) slow down the movement of electrons in a conductor. Under the BCS theory, movement of electrons in the superconductor lattice create perturbations in the wake, creating a very short-lived region of positive charge through lattice vibrations. The movement of the original electron is also affected. The positive charge then attracts a second electron whose movement is affected by the lattice vibrations caused by the first electron. The energy of a phonon created by the movement of the first electron has been transferred to the second electron and no energy is lost, the phonon is subsequently destroyed. In other words, no resistance is observed.

Experimental

Samples of CrSb, $CrSb_{1.02}$, $CrSb_{1.05}$, and $CrSb_{1.06}$ were made by the conventional solid-state method. Appropriately massed powders were added to an agate mortar and pestle and ground to ensure totally homogeneity for complete reaction. To eliminate unfavorable side reactions, the samples were sealed in evacuated silica tubes and placed into the furnace at 850°C for 24 hours at a 2°/min heating and cooling rate.

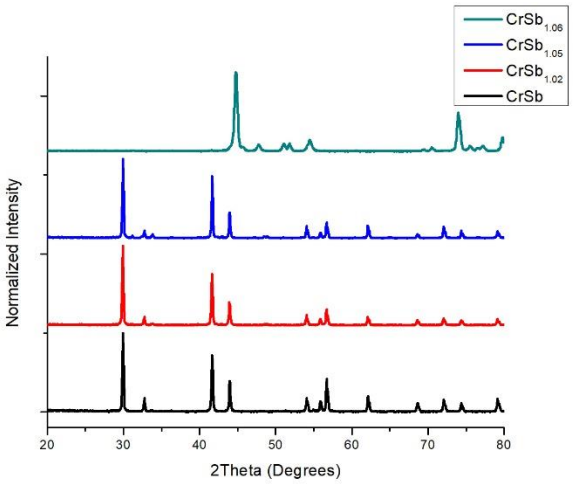

Figure 3: (Top) XRD patterns for CrSb (black), $CrSb_{1.02}$ (red), $CrSb_{1.05}$ (blue), and $CrSb_{1.06}$ (turquoise). A transition from the CrSb structure to $CrSb_2$ structure is observed from $CrSb_{1.05}$ and

Samples were characterized using a benchtop Rigaku miniflex diffractometer and CuKα x-ray source. A zero-background silicon crystal sample holder was used during XRD data collection for higher resolution.

Our $CrSb_{1.05}$ sample was sent to Dr. Arthur Ramirez at UC Santa Cruz for MPMS measurements.

Results/Discussion

Characterization of the series by XRD confirmed the NiAs type structure that crystallized in the $P6_3/mmc$ space group. CrSb, $CrSb_{1.02}$, $CrSb_{1.05}$, all crystallize in the same phase, whereas the increasing the atomic percentage of antimony to $CrSb_{1.06}$ leads to the formation of $CrSb_2$ as the main phase. Figure 3 shows the XRD patterns for the samples. The formation of $CrSb_2$ is supported by the phase diagram, where 50% atomic weight of antimony defines the phase boundary between CrSb and $CrSb_2$.[12] A whole pattern fitting method was employed in an attempt to confirm an expansion of the lattice parameter associated with the increased amount of Sb. However, the nominal amount is too small and the error present in our data collection does not allow for this determination. High resolution XRD or synchrotron data is necessary for analysis.

Figure 4 shows the magnetic data for $CrSb_{1.05}$ with an applied field of 1 kG. If a SC state was observed, we would expect to see a magnetic response similar to that of a perfect diamagnet—negative susceptibility due to the Meissner effect. However, from our data, it is very clear to see that no SC state is found. Our data represents more paramagnetic behavior similar to that of VSe with one major difference, that is, the molar susceptibility of our sample increases with temperature. Generally, the lattice vibrations brought on by thermal energy hinder magnetic ordering. In the case of Pauli paramagnetism which we may be observing in this case, delocalized spins in conducting materials align with the applied field, increasing ordering.

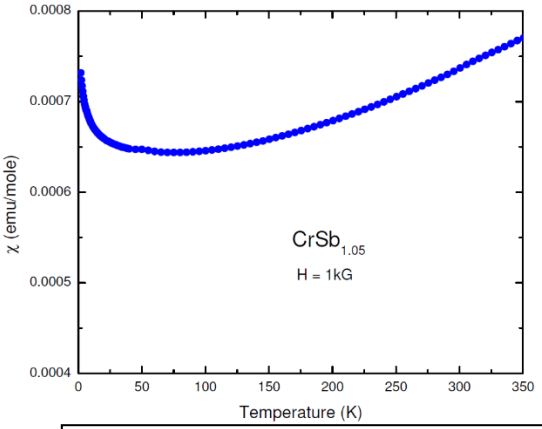

Figure 4: Magnetic data for CrSb1.05 in 1kG applied field. For a SC material, we would expect a negative susceptibility, no SC state is observed.

Even though a SC state was not found, research in superconducting states is important. Without specific structural attributes associated to superconductivity, only by making and testing samples can fruitful data be acquired. In the case of $CrSb_{1.05}$ we have found a spin stripe ordered material without a SC state. The greater implication of this research is that the spin stripe ordering is not necessarily linked to a SC phase.

4. Copper Substituted Magnesium Ferrite

Background

Solid solutions sometimes exhibit unpredictable behavior. The substitution of just one ion in the lattice can produce drastic differences in properties when compared to the parent compounds. Rational design of a solid solution is described by the Hume-Rothery rules. From greatest to least importance: (1) radii between substituted ion and substituting ion should not exceed ~15%, (2) the crystal structures of the two parent compounds must be isostructural, (3) similar valency should exist between substituting and substituted ions, and (4) similar electronegativity between the ions.[13]

CN	Cu^{2+}	Mg^{2+}	Fe^{3+}
t_d	0.57Å	0.57Å	0.49Å
O_h	0.73Å	0.720Å	0.645Å

Figure 5: Radii of Cu^{2+}, Mg^{2+}, and Fe^{3+} in different coordination environments[14]

Magnesium ferrite ($MgFe_2O_4$) is used for application as writable magnetic media. The structure adopts the spinel type and crystallizes in the Fd-3m space group. The spinel structure is characterized by the general formula AB_2O_4 in which divalent A atoms occupy 1/8 of the tetrahedral positions of a CCP oxygen framework and trivalent B atoms occupy 1/2 of the octahedral positions. Magnesium ferrite exists in what is known as an inverse spinel with fractional inversion. In a typical inverse spinel, A and B atoms swap positions so that the divalent A atoms reside in 1/4 of the octahedral positions and trivalent B atoms occupy the tetrahedral positions. Magnesium ferrite crystallizes with magnesium ions occupying both tetrahedral and octahedral positions (approximate 15% and 42% occupancy, respectively).[14]

Following the Hume-Rothery rules, facile substitution between $MgFe_2O_4$ and $CuFe_2O_4$ should be achievable. The ionic radii of Cu^{2+} and Mg^{2+} in tetrahedral coordination is identical while the difference in radii in octahedral coordination is less than 2%.[15] The radii are given in Figure 5.

Copper ferrite ($CuFe_2O_4$) may exist in 2 different space groups—cubic Fd-3m or tetragonal $I4_1/amd$. Both crystal structures exemplify complete copper filling of 1/4 of the octahedral positions. The cubic phase is stable only at high temperature and the difference in the cubic and tetragonal structures arises due to elongation of the octahedra from Jahn-Teller distortion, lengthening the cell along the c-axis. Stabilizing the cubic phase at room temperature requires quenching.

The Kramers model for superexchange can explain the ferromagnetic response associated with the magnesium ferrite structure. Adjacent edge-shared FeO_6 octahedra allow a bonding angle of 90°, providing FM behavior. Mg^{2+} ions are diamagnetic, so there will be no contribution to magnetism from this ion.

Experimental

Samples of $Mg_{1-x}Cu_xFe_2O_4$ were made by the conventional solid-state method. Starting materials are CuO, MgO, and Fe_2O_3. Appropriately massed powders were added to an agate mortar and pestle and ground to ensure totally homogeneity for complete reaction. Pellets were pressed using a cold isostatic press. For x=0 to x= 0.9, samples were heated at 1100°C for 12 hours at a 5°/min heating and cooling rate. For x=1 ($CuFe_2O_4$), this sample was heated to 1000°C for 24 hours to prevent melting with the same heating/cooling profile.

Samples were characterized using a benchtop Rigaku miniflex diffractometer and CuKα x-ray source. A zero-background silicon crystal sample holder was used during XRD data collection for higher resolution.

Samples of x=0, x= 0.5, and x=0.7 were used for MPMS measurements.

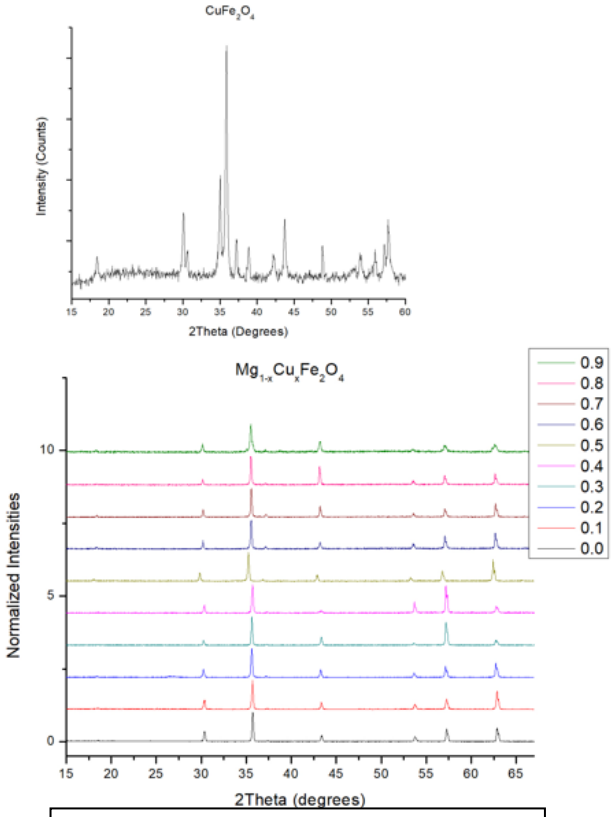

Figure 6: (Bottom) patterns for $Mg_{1-x}Cu_xFe_2O_4$; x= 0 to 0.9. All patterns fit the cubic Fd-3m space group. (Top) XRD pattern for $CuFe_2O_4$ fits the $I4_1/amd$ space group. The phase transition must exist between x= 0.9 and 1

Results/Discussion

Characterization of the samples by XRD were conducted for phase identification. Subsequent patterns were fit to the Fd-3m space group. It can be clearly seen from figure 6 that the addition of copper into the magnesium ferrite structure does not affect the cubic structure through x= 0.9. Only at the parent compound (x= 1) do we see the emergence of the $I4_1/amd$ space group. Whole pattern fitting was employed to determine lattice parameter for x= 0, 0.1, 0.5, and 0.7. It is found

that the lattice parameter decreases with increasing copper substitution and becomes stagnant between x=0.5 and 0.7. This is a deviation from Vegard's rule, which ultimately states that substitution of a larger ion increases the lattice parameter in a linear fashion.[16] Vegard's rule, however, is not a definitive law, and deviations commonly occur.

The similar radii of Mg^{2+} and Cu^{2+} creates difficulty in whole pattern fitting if copper only replaces magnesium. However, the fact that a difference can be observed between fitting XRD patterns suggests that the replacement of Fe^{3+} by Cu^{2+} is also occurring, figure 7. Without high resolution data, the effect of copper substitution magnesium cannot be accurately determined. Rietveld analysis is required for deeper insight. The Shannon radii of Cu^{2+} is larger than Fe^{3+} but the difference in electronegativity may be the reason for a decreasing cell volume.

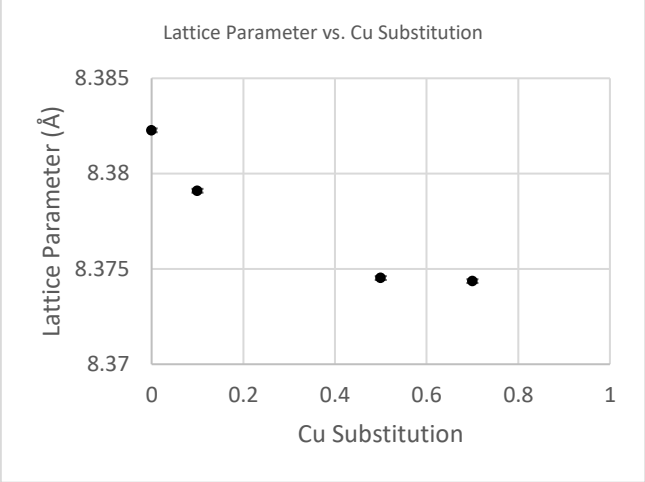

Figure 7: Lattice parameter decreases with increasing copper substitution up until x= 0.5, a deviation from Vegard's rule. This suggests substitution of both Fe^{3+} and Mg^{2+} by Cu^{2+}

Magnetic measurements for x= 0, 0.5, and 0.7 are presented in figure 8. The profiles show ferromagnetic behavior stemming from the 90° superexchange occurring between adjacent octahedra. As the degree of copper substitution increases, we observe an increase in the magnitude of magnetic susceptibility. This can be owed to an increased number of unpaired spins from Cu^{2+} substituting Mg^{2+}. Magnesium will not contribute to magnetic response, so the only mechanism for ferromagnetism is filling of the octahedral position with either copper or iron cations. The e_g orbitals (d_{z2}, d_{x2-y2}) of Fe^{3+} contain two unpaired electrons while Cu^{2+} contains only 1 unpaired electron, thus, we would expect a slightly decreased susceptibility if copper solely replaced iron. The data suggests the substitution of $Mg^{2+}$by Cu^{2+} in the octahedral position. Further investigation of the ion occupancies at the tetrahedral and octahedral positions is required for more definitive evidence. Furthermore, the phase transition between x= 0.9 and 1 should be probed and tested for magnetic response at the phase boundary, as Jahn-Teller distortions may simultaneously elongate the c lattice parameter and shorten the cell in the a-b plane, allowing higher degrees of orbital overlap. This study has shown an increase in the magnetic susceptibility of $MgFe_2O_4$ by Cu^{2+} substitution.

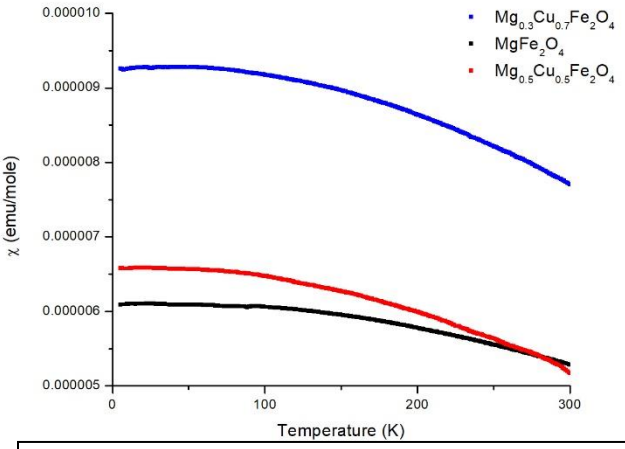

Figure 8: Magnetic data for $MgFe_2O_4$, $Mg_{0.5}Cu_{0.5}Fe_2O_4$, and $Mg_{0.3}Cu_{0.7}Fe_2O_4$. Magnetic susceptibility increases with copper content

Conclusion

VSe, $CrSb_{1.05}$, and copper substituted magnesium ferrite were studied using magnetic data. It was found that VSe was highly frustrated but showed no definitive evidence of ordering. $CrSb_{1.05}$ did not exhibit the Meissner effect characteristic of superconducting phases, nevertheless, it is impossible to pre-emptively determine the presence of a superconducting state with current methods. Only through synthesis and testing can we provide evidence (or lack thereof) of superconductivity. Copper substituted magnesium ferrite was found to have an increased molar susceptibility with increasing degree of substitution.

References

(1) Goodenough, J. B. *Magnetism and the Chemical Bond*; 1963.

(2) Tsubokawa, I. On the Magnetic Properties of Vanadium Sulfide and Selenide. *J. Phsical Soc. Japan* **1959**, *14* (2), 196–198. https://doi.org/10.1143/JPSJ.54.3018.

(3) Yamashita, J.; Kondo, J. Superexchange Interaction. **1958**, *28* (1953).

(4) Diep, H. T. Phase Transition in Frustrated Magnetic Thin Film-Physics at Phase Boundaries. *Entropy* **2019**, *21* (2), 1–43. https://doi.org/10.3390/e21020175.

(5) Diep, H. T. Theoretical Methods for Understanding Advanced Magnetic Materials: The Case of Frustrated Thin Films. *J. Sci. Adv. Mater. Devices* **2016**, *1* (1), 31–44. https://doi.org/10.1016/j.jsamd.2016.04.009.

(6) Uchino, K. *Advanced Piezoelectric Materials: Science and Technology*; Elsevier: Duxford, 2017.

(7) Subramanian, M. A. *CH513 Course Notes*; 2018.

(8) Dahal, A.; Gunasekera, J.; Singh, D. K. Possible Superconductivity in Chemically Doped $CrSb_{1+\delta}$. *Phys. status solidi - Rapid Res. Lett.* **2017**, *11* (10), 1700211. https://doi.org/10.1002/pssr.201700211.

(9) F., S. R. Could Charge Stripes Be a Key to Superconductivity? *Science (80-.).* **1999**, *283* (4504), 1106–1108.

(10) Ivashko, O.; Yang, L.; Destraz, D.; Martino, E.; Chen, Y.; Guo, C. Y.; Yuan, H. Q.; Rønnow, H. M.; H, M.; Matus, P.; et al. Charge-Stripe Order and Superconductivity in ArXiv : 1708 . 06537v2 [Cond-Mat . Supr-Con] 27 Nov 2017. 1–8.

(11) Emery, V. J.; Kivelson, S. A.; Tranquada, J. M. Perspective Stripe Phases in High-Temperature Superconductors. **1999**, *96* (16), 8814–8817.

(12) Venkatraman, M.; Neumann, J. P. The Cr-Sb (Chromium-Antimony) System. *Bull. Alloy Phase Diagrams* **1990**, *11* (5), 435–440.

(13) Science, S. N. L. for M. *Hume-Rothery-Rules*; 2016.

(14) Antao, S. M.; Hassan, I.; Parise, J. B. Cation Ordering in Magnesioferrite, MgFe2O4, to 982 °C Using in Situ Synchrotron X-Ray Powder Diffraction. *Am. Mineral.* **2005**, *90* (1), 219–228. https://doi.org/10.2138/am.2005.1559.

(15) Shannon, R. D. Revised Effective Ionic Radii in Halides and Chalcogenides. *Acta Crystallogr.* **1976**, No. A32, 751. https://doi.org/10.1107/S0567739476001551.

(16) Denton, A. R.; Ashcroft, N. W. Vegards Law. *Phys. Rev. A* **1991**, *43* (6), 3161–3164. https://doi.org/10.1103/PhysRevA.43.3161.